International Scientific Colloquium
Modelling for Material Processing
Riga, June 8-9, 2006

Mathematical Modelling of Sintering of SiO_2 Crucibles

U. Bethers, J. Sennikovs, H. Szillat, A. Timuhins, J. Virbulis

Abstract

Mathematical model of the sintering process is applied to determine the shape distortion of the ceramic crucibles during sintering. The parameters of the model are determined from the series of experiments during which the shrinkage of the SiO_2 material was measured.

Introduction

Sintering of the porous material is a process that leads to its compaction when the particles adhere to each other. The heat is applied to material during the process of sintering. It is the last stage in manufacturing of ceramic materials. During the sintering ceramic material acquires its final flexural strength and, therefore, it is one of the most important parts of the whole process of manufacturing of ceramics. Sintering process is characterised by changes of microstructure of the material, as well as by macroscopic shrinkage and shape distortion.

The present paper applies continuum model of sintering to the final stage of manufacturing of the SiO_2 crucibles used in production of solar panels. The crucibles are made from fused silica by pressure casting of silica slurry, pre-dried, and sintered at temperature around 1250 °C. The particular crucibles are of rounded-rectangular shape and therefore are more vulnerable to the structural deformations than round ones.

The work presented here consists of

(1) experimental part during which the dependence of the shrinkage of the material on the applied thermal load is determined,

(2) application of the mathematical model of sintering to predict the time-development of shrinkage of the material for particular thermal forcing,

(3) application of 3D mathematical model to calculate the shape deformations of real crucibles.

1. Theory

The mathematical model of the sintering was formulated in the macroscopic approach [1] following the rheological theory of the sintering introduced in [2]. The theory is based upon the concept of the generalized – viscous flow of porous bodies.

The sintering (creep) strain is introduced in the stress-strain equation as

$$\sigma = D\left(\varepsilon^{tot} - \varepsilon^{S}\right) \qquad (1)$$

here σ is stress tensor, $\varepsilon^{\mathrm{tot}}$ is total strain, and ε^{S} is sintering strain. The constitutive equation for the linear viscous incompressible material with voids is [1,3]

$$\dot{\varepsilon}_{ij}^{S} = \frac{\sigma'_{ij}}{2G} + \frac{\left(\sigma_{kk}/3 - P_L\right)}{3K} S_{ij} \tag{2}$$

where $\dot{\varepsilon}_{ij}^{S}$ is strain rate tensor due to the [inelastic, i.e. viscous] sintering, (dot over the symbol hereafter denotes time derivative), P_{L} is the sintering stress, G and K are, respectively, effective shear and bulk viscosity coefficients and σ'_{ij} is the deviatoric part of the stress tensor

$$\sigma'_{ij} = \sigma_{ij} - \delta_{ij}\sigma_{kk}/3 \tag{3}$$

Sintering stress (or effective Laplace pressure P_{L}) for the porous bodies is defined [1]:

$$P_L = P_{L_0}\left(1-\theta\right)^2 = \frac{3\alpha}{r_0}\left(1-\theta\right)^2 \tag{4}$$

Here material properties α is the surface tension and r_0 is the typical radius of the material particles. Porosity θ is given as the ratio of the void volume to the total material volume, and it is in essence the model parameter calculated from

$$\dot{\theta} = \left(1-\theta\right)\cdot\dot{\varepsilon}_{kk}^{S} \tag{5}$$

The effective shear viscosity is also derived in [1] as

$$G = \eta_0\left(1-\theta\right)^2 \tag{6}$$

whilst effective bulk viscosity as

$$K = 2\eta_0\frac{2\left(1-\theta\right)^3}{3\theta} \tag{7}$$

Eqs. (6) and (7) contain the shear modulus η_0 of the porous body skeleton, and it is a function of temperature and porosity. The literature (for example [4]) suggests that

$$\eta_0 \sim r_0^3 f\left(\theta\right)T\cdot e^{\frac{E}{kT}} \tag{8}$$

Material property η_0 has to be evaluated from experiment.

2. Evaluation of model parameters from experiments

The experiments included sintering of the samples of two different raw materials used for production of the crucibles. Different sintering regimes were applied varying both the maximum (process) temperature (900-1350°C) and the sintering time (1-3 hours). Typical temperature time curves for experiments are shown in fig.1. The shrinkage of the samples at the end of process due to the sintering was measured.

For the evaluation of the shear modulus η_0 from the sintering experiments we use expression for the sintering rate that is obtained from eqs. (2), (4) and (7), assuming that conditions are isotropic:

$$\dot{\theta} = -\frac{3P_{L_0}}{4\eta_0}\theta \qquad (9)$$

We assumed that the sintering rate (i.e. change of porosity in time $\dot{\theta}$) is dependent on the temperature and the porosity θ itself

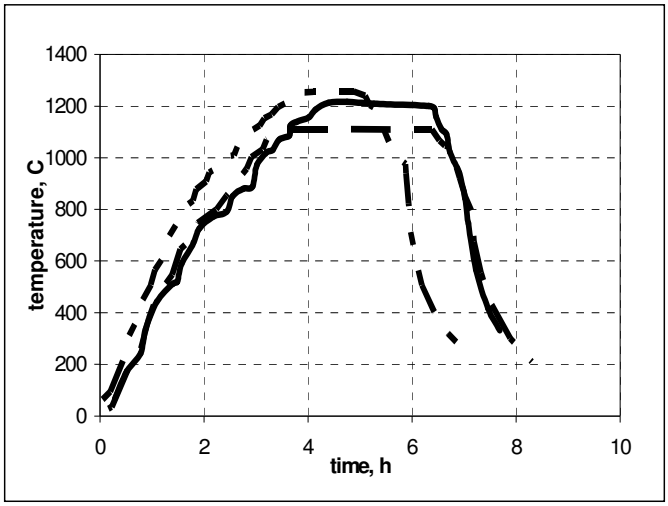

Fig. 1. Typical time-dependence of temperature during sintering experiments.

$$\dot{\theta} = -f(\theta)\frac{e^{-\frac{E}{kT}}}{T} \qquad (10)$$

and proposed an exponential dependency of the sintering rate on the porosity

$$f(\theta) = e^{-(\theta - B)/A} \qquad (11)$$

Only the final shrinkage of the samples was known, therefore we must use the integral representation of (10)

$$\int \frac{d\theta}{f(\theta)} = -\int \frac{e^{-\frac{E}{kT}}}{T} dt \qquad (12)$$

or, inserting (11) into (12) and integrating over the sintering thermal cycle

$$e^{\frac{\theta - B}{A}} = -\int_t \frac{e^{-\frac{E}{kT}}}{T} dt = \varphi \qquad (13)$$

The integral on the right-hand-side of (13) can be calculated from the experimental data log; we used the least square method to determine the model parameters A, B and E from the experiment results. The linear fitting in

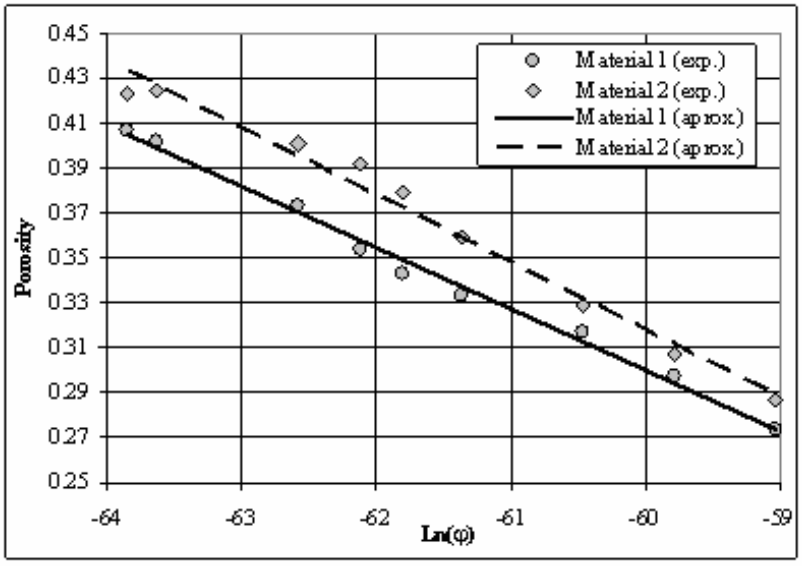

Fig. 2. Experimental (dots) and linear theoretical (lines) dependency of the sample porosity θ on the time integral $\ln(\varphi)$

the axis $(\ln\varphi)-(\theta)$ is shown in Fig. 2.

Thus, we have experimentally obtained the dependence of the shear modulus η_0 on the temperature and porosity as

$$\eta_0(\theta,T)=\frac{3\theta P_{L_0}}{4}\frac{e^{\frac{\theta-B}{A}}}{A}e^{\frac{E}{KT}}T \qquad (14)$$

3. Results of modelling

The time-development of shrinking is determined solving the equation (9). The time-dependence of porosity in this case is determined by the time-dependence of temperature.

Solution of this time-rate equation for porosity for all experiments, and comparison of the final sample porosity with the model result is presented in Fig. 3. One may notice good agreement between the experimental results and the del predictions.

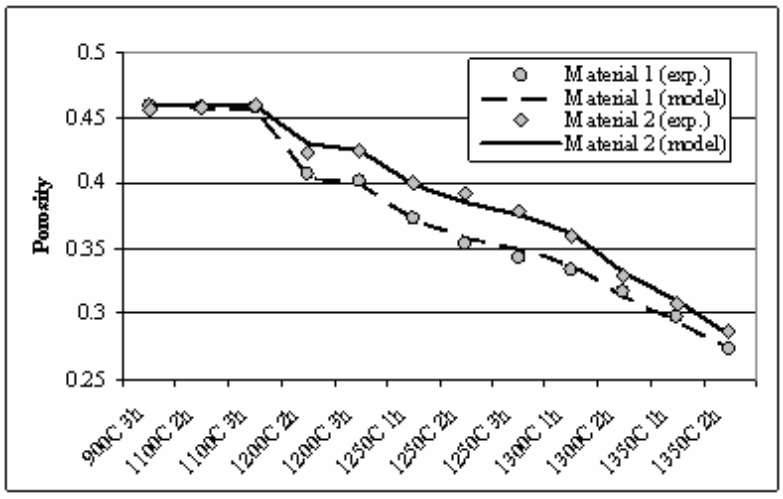

Fig. 3. The measured (dots) and modelled (lines) sample porosities for the sintering experiments.

Another example is the calculation of the time development of the (SiO_2 sample) porosity prescribing different thermal cycles, i.e. the time development of the process temperature. Fig. 4 illustrates the effect of the application of three different process temperatures (1210, 1240 and 1270° C). All three thermal cycles are similar: (a) temperature increase by 10 K/min up to 1100° C, (b) temperature increase by 2 K/min up to process temperature and (c) holding of the process temperature for some process time, (d) temperature decrease by 15 K/min. We adjusted the process time for three sintering cycles to equalize the temperature integral φ, see Eq. (13). One may consider that the resulting sintering level (porosity) is the

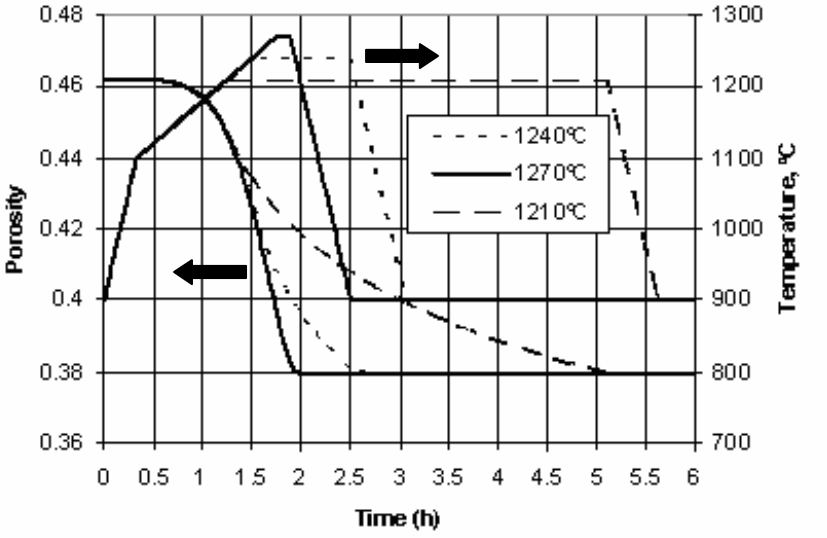

Fig. 4. Modelling of the time development of the porosity. Variation of the process temperature.

same – only it is achieved by process time 15 min @ 1270° C, 1h @ 1240° C or 4h @ 1210° C. Fig. 4 also shows the qualitative behaviour of the sintering process (a) higher sintering rate at higher temperatures, (b) decrease of the sintering rate with the increase of the sintering level.

The finite element model of temperature, porosity, stresses and deformations has been applied to calculate the shape deformation of the crucible. The typical setup of the sintering furnace and temperature distribution in the furnace is shown in fig. 5. The calculated temperature difference between the different parts of the crucible during the main process phase is few degrees. Therefore the stresses induced by different sintering rates caused by temperature inhomogeneity are small.

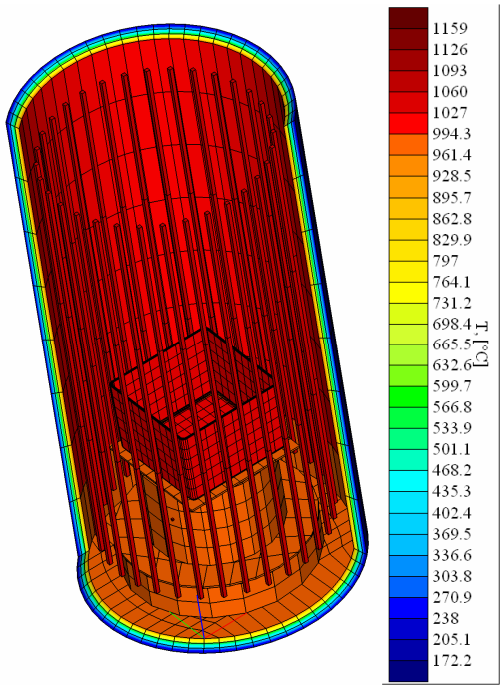

Fig. 5. Typical sintering furnace setup and temperature distribution in furnace.

Fig. 6 illustrates crucible shape distortions, crucible size is 460 mm. The side view indicates almost uniform settling (shrinkage) of the crucible and the slight outwards bending of the side walls in the vertical cross section. The top view shows the main distortion of the crucible upper perimeter. The vertical displacement of the crucible is rather trivial, and corresponds to approx. 6% material shrinkage for the end stage. The development of the distribution of the horizontal displacements is a combination of the overall material shrinkage and the shape distortion of the crucible. The bottom part of the crucible does not suffer from the shape distortion: the moving of the inner bottom perimeter towards the center corresponds to approx. 5% shrinkage. This is slightly less than 6% settling due to the lower sintering level of the bottom perimeter exposed to a higher tensile stress. The horizontal displacement of the central part of the vertical walls is a combination of the material shrinkage with the outward (convex) bending of the side walls. Note, that this shape-distorting effect is characteristic not only for the upper but also (and, expecially, during the initial phase of deformation) for the central part of the side walls. One may consider that the upper edge moves toward the crucible centre; efficiently, the initially nearly-rectangular upper perimeter distorts, and becomes rounded. This shape distortion effect increases with the development of the sintering process. Thus, we may consider that the main problem in the adjusting the parameters of the sintering process is related to the avoiding of the characteristic shape distortion of the crucible.

Conclusions

- The model of the sintering process allows determination of the sintering level of the raw material as a function of the applied thermal cycle. The final porosity of the material is given as a function of the thermal cycle parameters (process temperature and duration)
- The temperature non-uniformity has minor effect on the non-uniformity of the sintering and on the development of the tensile stresses.
- The inner bottom perimeter, and, especially, inner bottom corners have essentially lower final sintering level due to they are exposed to the tensile stress which reduces the sintering rate.

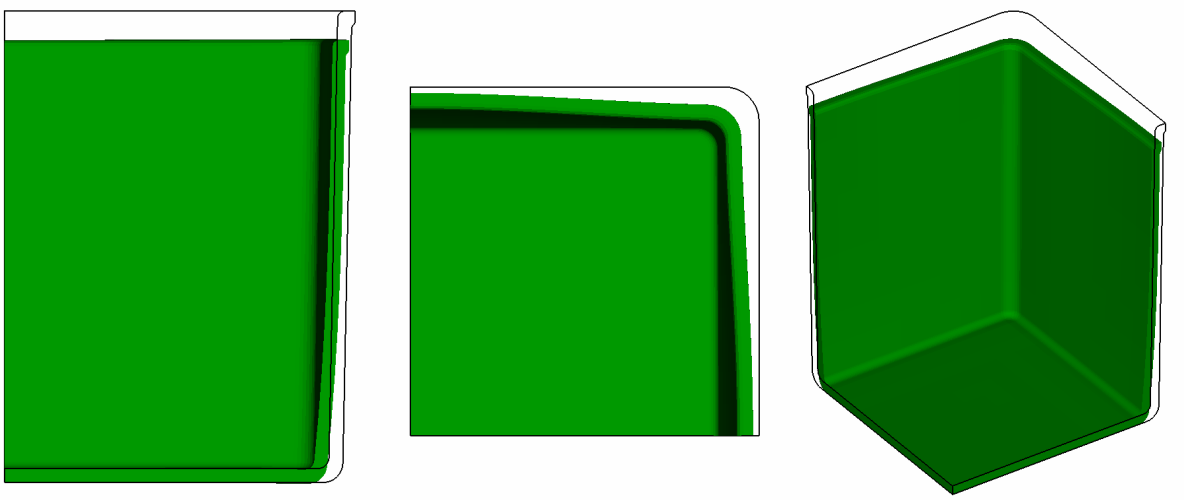

Fig. 6. Side, top and isometric views of the crucible shape distortion during the sintering process. One quarter of crucible is shown.

- The shape distortion of the crucibles during the sintering process is characteristic with (1) the outwards bending of the central and upper parts of the vertical side walls and (2) rounding of the initially rectangular upper crucible perimeter.

Acknowledgement

We acknowledge prof. Rūdolfs Cimdiņš (Riga Technical University) for conducting sintering experiments used in this paper.

References

[1] Olevsky, E. A., *Theory of Sintering: From Discrete to Continuum*, Materials Science and Engineering, R23, 1998, pp. 41-100, 1998.

[2] Skorohod, V. V. *Rheological basis of the theory of sintering*. Naukova Dumka, Kiev, 1972.

[3] Kraft, T. & Riedel, H. *Numerical simulation of solid state sintering: model and application*. J. of the European Ceramic Society 24, 2004, pp. 345-361.

[4] Argüello, J. G., Tikane V., Garino, T. J. & Braginsky, M. V. *Three-dimensional simulation of sintering using a continuum modeling approach*, Sintering 2003, 2003

Authors

Dr.-Phys. Bethers, Uldis
Sennikovs, Juris
Timuhins, Andrejs
Dr.-Phys. Virbulis, Janis
Center for Processe Analysis and Research
Zellu str. 8, LV-1002 Riga, Latvia
E-mail: jsenniko@latnet.lv

Dr.Szillat, Holger
Wacker Chemie GmbH.
Johanness-Hess-Strasse 24
D-84489, Burghausen, Germany